THE OFFICIAL MAGAZINE OF THE OCEANOGRAPHY SOCIETY

Oceanography

Light Absorption by Phytoplankton, Non-Algal Particles, and Dissolved Organic Matter in San Jorge Gulf in Summer

By Gabriela N. Williams, Pierre Larouche, Ana I. Dogliotti, and Maité P. Latorre

COASTAL COMPLEXITY. Composite satellite image of the San Jorge Gulf and adjacent ocean taken on February 14, 2014, (MODIS Aqua sensor) on Google Earth Pro during the MARES fieldwork program. The red-green-blue (667 nm, 531 nm, 443 nm) image shows the complex sea color spatial patterns resulting from the presence of phytoplankton, detritus, and dissolved organic matter. *Credit: NASA Goddard Space Flight Center, Ocean Ecology Laboratory, Ocean Biology Processing Group. Image processed by Nora Glembocki using SeaDAS*

ABSTRACT. San Jorge Gulf (SJG) along the Atlantic coast of South America is of high ecological importance, a place where several industrial fisheries exploit species such as hake, the Argentine red shrimp, and the Patagonian scallop. In this region, phytoplankton distribution is often related to bathymetric or oceanographic features such as capes, upwellings, and frontal areas that drive the renewal of nutrients in the surface layer. Satellite remote sensing is a key tool for monitoring such a large ecosystem. Knowledge of the optical properties of seawater in this area is necessary to assess the quality of operational ocean color products. Absorption of light by phytoplankton (a_{phy}), non-algal particles (a_{NAP}), and colored dissolved organic matter (a_{CDOM}), as well as the concentration of chlorophyll-a were measured in February 2014 in the surface layer of the SJG. These parameters all exhibited strong spatial variability that resulted from the gulf's large-scale circulation and bathymetric features. Although CDOM dominated the absorption budget, there was good correlation between a_{CDOM} and a_{phy}, leading to the characterization of San Jorge Gulf as "Case-1" waters where remote-sensing algorithms should perform well. Study results showed that the phytoplankton composition was mainly dominated by small cells (0.2–2 μm, i.e., picophytoplankton). The $a_{phy}^{*}(440)$ measured at the end of summer in the SJG (0.01–0.08 $m^2\,mg^{-1}$) are in a similar range to those observed elsewhere. Particulate absorption was dominated by phytoplankton (66%).

INTRODUCTION

Satellite remote sensing of ocean color aims primarily at assessing chlorophyll-a (Chla) concentration in the global ocean. Ocean color is determined by seawater's inherent optical properties (IOPs; Preisendorfer, 1976), with Chla being just one of the active components that influence IOPs. Therefore, Chla concentrations determined from ocean color remote sensing have larger uncertainties than the IOPs themselves. Variations in IOPs are clear indications of changes in water mass or water constituents. Increased knowledge of the spatial and temporal variability of the optical properties can optimize the use of ocean color remote sensing and eventually provide improved and reliable products related to ocean biogeochemistry (IOCCG, 2006).

IOPs alter the penetration of solar radiation through absorption and scattering, and thus influence light-related processes such as photosynthesis (Astoreca et al., 2012). The reflected light contains a wealth of information regarding absorption and scattering by the particulate and dissolved constituents, and by the water itself (Roesler and Perry, 1995).

The spectral total absorption coefficient of seawater, $a_t(\lambda)[m^{-1}]$, can be subdivided into four additive components (Prieur and Sathyendranath, 1981; Carder et al., 1991):

$$a_t(\lambda) = a_w(\lambda) + a_{phy}(\lambda) + a_{NAP}(\lambda) + a_{CDOM}(\lambda).$$

These components account for the contributions of pure seawater (a_w), phytoplankton (a_{phy}), non-algal particles (a_{NAP}) or detritus, and colored dissolved organic matter (a_{CDOM}) also called "gelbstoff."

The San Jorge Gulf (SJG) region along the Atlantic coast of South America has significant biological importance. Several economic activities take place there, including three industrial fisheries: hake (*Merluccius hubbsi*, Marini 1933), Argentine red shrimp (*Pleoticus muelleri*, Bate 1888), and the Patagonian scallop (*Zygochlamys patagonica*). Phytoplankton serve as the food web base in the ocean and, through the organic matter they produce, fuel marine ecosystems. Phytoplankton are thus a valuable indicator of ecosystem state. In this biologically important region, phytoplankton are known to grow in patches that are often related to bathymetric or oceanographic features, such as capes or upwelling and frontal areas (Gagliardini and Colón, 2004; Glembocki, 2015), which drive nutrient renewal in the surface layer. These areas have also been associated with the location of the Patagonian scallop fishing grounds (Bogazzi et al., 2005). Tidal fronts in the northern and southern SJG (Akselman, 1996; Carreto et al., 2007; Fernández, 2006; Rivas and Pisoni, 2010; Glembocki et al., 2015) have been associated with relatively high Chla concentrations throughout spring and summer, as identified by ocean color remote sensing methods (Acha et al., 2004; Rivas, 2006; Carreto et al., 2007; Romero et al., 2006; Glembocki et al., 2015). In situ studies also found high surface Chla concentrations (14.00 mg m^{-3}) in spring (Cuchi Colleoni and Carreto, 2001). Some more recent studies focused on the variability of absorption coefficients in the Southwestern Atlantic and Southern Oceans at one coastal station (Lutz et al., 2006), in the Patagonian Shelf Break Front, and in adjacent areas (Garcia et al., 2005; Ferreira et al., 2009, Segura et al., 2013b), and along the Magellan Strait (Lutz et al., 2016).

This study analyzes a series of bio-optical measurements collected from the SJG to determine the contributions of the main surface-water components (i.e., phytoplankton, detritus, and colored dissolved organic matter) in summer. Its objective is to increase understanding of phytoplankton absorption properties in Argentinean marine coastal waters.

MATERIAL AND METHODS
Study Area

The SJG is a semi-open basin with an area of 39,340 km^2 located between 45°S (Cape Dos Bahías) and 47°S (Cape Tres Puntas), and between 65°30'W and the coast of Argentine Patagonia (Figure 1). The basin's central region, delimited by the 90 m isobath, has a maximum depth of 110 m near its center. SJG waters communicate with the adjacent shelf over a distance of approximately 250 km, at depths ranging from 90 m in the north and center to 50–60 m at the south end, where there is a pronounced sill known by fishermen as "La Pared" (Spanish word for The Wall). No rivers flow into the gulf, and precipitation is scarce (average of

233 mm yr^{-1} in Comodoro Rivadavia), so continental input is negligible. Bottom sediments in the central gulf, a depositional environment, are dominated by fine silt rich in organic carbon derived from seasonal high phytoplankton primary production in the upper layer of the water column (Fernández et al., 2003, 2005; Fernández, 2006). The oxygen concentration in near-bottom water is consistently lowest in the central basin (Fernández et al., 2005).

The so-called Patagonian Shelf Water, including that of the SJG, is a mixture of subantarctic water carried by the Cape Horn Current and low-salinity, low-temperature water from the Magellan Plume (Figure 1c). The latter, formed by discharge from Magellan Strait, extends along the inner shelf of southern Patagonia and enters the southeast sector of the SJG (arrow in Figure 1c) around Cape Tres Puntas (Acha et al., 2004;

Palma and Matano, 2012). In adjacent shelf waters, the axis of the plume follows the 100 m isobath, which shifts offshore at the latitude of the SJG. Modeling results indicate that during summer there is a wide cyclonic coastal current system and a recirculating cyclonic gyre in the southern sub-basin. Tides and winds are the main forcing mechanisms of the circulation (Matano and Palma, 2018, in this issue).

Sampling Strategy

The data were collected during the MARES (MArine ecosystem health of the San Jorge Gulf: Present status and RESilience capacity) expedition between January 29 and February 15, 2014. Sampling included a high spatial resolution survey of the southern frontal region (15 F stations), a time series in the center of the SJG mouth (15 SFx stations), a grid (16 G stations) covering the whole SJG (Figure 1b,c), and

a station (T09) in the center of the gulf. At each station, discrete samples for Chla and IOPs were collected from the surface and at selected depths, based on the fluorescence profile. Only surface data will be presented for this study, as other samples were too deep to contribute significantly to the light detected by satellite sensors.

Chlorophyll-*a* Concentration

Samples for in situ Chla determination were collected by filtering 500 ml of seawater through 47 mm Whatman GF/F filters. The filters were stored at −80°C until analysis at the Institut des Sciences de la Mer de Rimouski. Chla was extracted with 90% acetone and measured with a Turner Designs fluorometer, according to Strickland and Parsons (1972).

Phytoplankton Density

Surface water samples were preserved in Lugol (4%, 4°C in the dark) for microphytoplankton (≥20 μm and ≤200 μm) enumeration, following the Utermöhl (1958) method, with a Zeiss Axiovert 100 inverted microscope. Taxonomic identification was done following Tomas (1997). A second surface water sample was preserved in glutaraldehyde 25% (0.1% final concentration, −80°C) for cytometry analysis using an EPICS ALTRA flow cytometer (Beckman Coulter Inc.) equipped with a 488 nm laser (15 mW output), following Tremblay et al. (2009). The flow cytometer allows classifying phytoplankton by cell size using auto-fluorescence to estimate the angle of light scattering (Collier, 2000). Use of this method allows detection of cells like picophytoplankton (0.2–2 μm in size) and nanophytoplankton (2–20 μm in size) and their classification according to pigmentation as prokaryotes (pico- and nanocyanobacteria) and eukaryotes (pico- and nanoeukaryotes).

Colored Dissolved Organic Matter Absorption

Due to logistical constraints on the ship, seawater samples were filtered through 0.2 μm Anotop filters (acid pre-washed), and the filtrate was kept in glass bottles
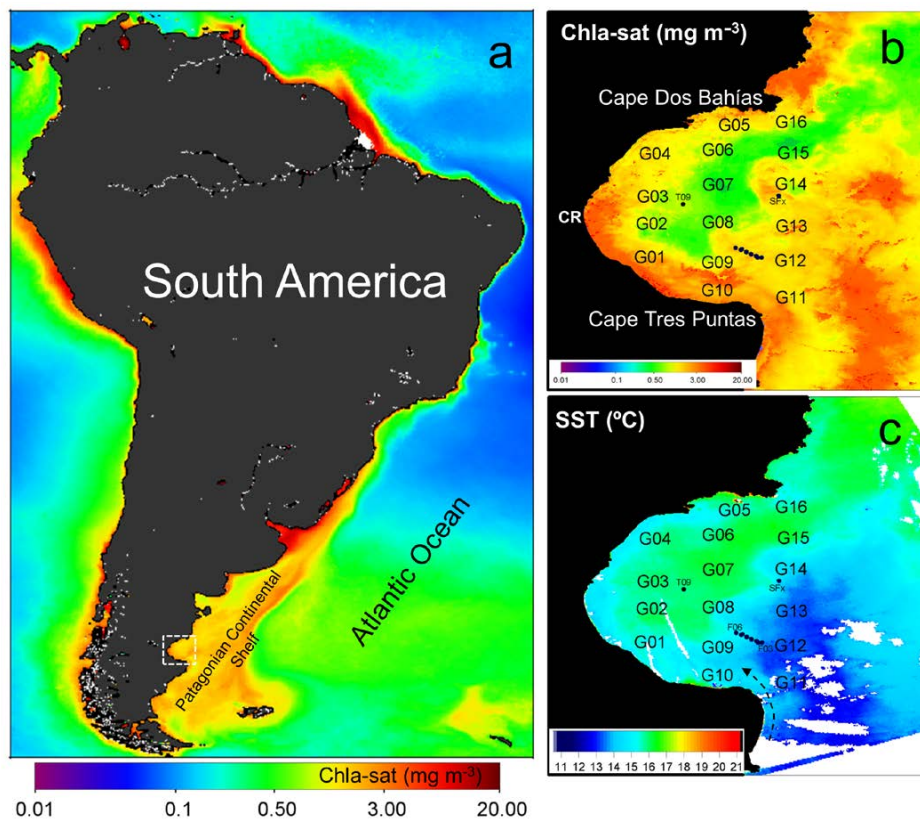
FIGURE 1. (a) MODIS chlorophyll-*a* (Chla-sat) 2003–2016 climatology showing the location of the study area. Locations of sampled stations overlaying MODIS Aqua average images of (b) Chla-sat, and (c) sea surface temperature (SST) for the period January 30 to February 15, 2014. CR = Comodoro Rivadavia city. The arrow in (c) indicates the pathway by which coastal waters of the Magellan Plume enter San Jorge Gulf.

at −20°C for no longer than six months before analysis. Although freezing is not recommended for oceanic samples (Nelson and Coble, 2009), there is no consensus on CDOM long-term storage. Some studies showed decreases in CDOM absorption (Spencer et al., 2007; Hudson et al., 2009), while others found minimal effects of freezing on DOM (Spencer and Coble, 2014, and references therein). Hancke et al. (2014) showed that neither a_{CDOM}(350) nor the slope coefficient (S) depend on frozen sample storage duration up to 120 days.

After thawing and acclimation to room temperature, CDOM optical density was measured between 250 nm and 800 nm using 10 cm cuvettes in a single-beam spectrophotometer (HP8452 diode array) in the Laboratorio de Oceanografía Química y Contaminación de Aguas (CESIMAR-CENPAT). Ultra-pure water (OSMOION UV system) was used as a blank. The value of optical density at 600 nm was subtracted from the whole spectrum. Absorption coefficients for CDOM, $a_{CDOM}(\lambda)$ [m^{-1}], were estimated by using the conversion factor to go from decimal to natural logarithms and by accounting for the cuvette pathlength.

Particulate Absorption
Seawater samples were filtered on board onto GF/F glass fiber filters at dim light and low pressure (<35 kPa). Filters were kept at −80°C until measurement in the laboratory. Optical density of the total particulate material was measured between 350 nm and 800 nm in a double beam Shimadzu UV-210A spectrophotometer following the quantitative filter technique (Mitchell, 1990) at the Producción Primaria y Biotoxicidad laboratory of the Instituto Nacional de Desarrollo Pesquero (INIDEP) in Argentina. Filters were then washed with methanol and the optical density of detritus was recorded (Kishino et al., 1985). Optical density values averaging between 790 nm and 800 nm were subtracted from the whole spectrum in each case (total and detritus). Spectra

were corrected for pathlength amplification factor by applying the quadratic equation of Mitchell (1990) using the coefficients reported by Hoepffner and Sathyendranath (1992). Total particulate ($a_p(\lambda)$), detritus ($a_{NAP}(\lambda)$), and phytoplankton ($a_{phy}(\lambda) = a_p(\lambda) - a_{NAP}(\lambda)$) absorption coefficients [m^{-1}] were estimated by using the conversion factor to go from decimal to natural logarithms for the filter area and for seawater volume filtered (Mitchell and Kiefer, 1988). The blank consisted, in each case, of a glass fiber filter through which a volume of pre-filtered surface seawater similar to that of the sample was filtered.

REMOTE-SENSING DATA
Mean images from MODIS (Moderate-Resolution Imaging Spectroradiometer) Aqua Chla (Chla-sat) and sea surface temperature for the period January 30 to February 15, 2014, were calculated using Level 2 NASA standard products at 1 km resolution to show the average oceanographic conditions during the cruise period (Figure 1b,c). The standard Chla product derived from the OC3M algorithm was used (updated version after 2013 reprocessing). Also, eight-day composite level-3 images of Chla-sat, a_{phy}, and $a_{NAP+CDOM}$ were retrieved from the NASA ocean color web page (http://oceancolor.gsfc.nasa.gov/cgi/l3). It is a nominal 4 km resolution product generated with the OC3Mv5 algorithm and the Generalized Inherent Optical Property (GIOP) model. These data were extracted over the study area (44°30'–47°30'S and 68°00'W–64°00'W) and re-gridded to a Geographic Lat/Long WGS84 projection at 0.03331° × 0.033311° resolution.

To analyze the long-term temporal variability of Chla-sat, a_{phy}, and $a_{CDOM+NAP}$ (non-algal particle colored dissolved organic matter) at 443 nm for the study area, mean monthly data were generated by arithmetically averaging all MODIS level-3 eight-day images retrieved from the Giovanni web page (https://giovanni.gsfc.nasa.gov/giovanni/) for the period January 2003–May 2016.

Statistical Analyses
The variability of each optical parameter was examined by calculating the mean, maximum, and minimum values along with the standard deviations (SDs) and variation coefficients. Correlation coefficients between two different variables were calculated with p-value using an analysis of variance (ANOVA). Because there were no replicate data to obtain error estimates, it was assumed that all points had similar sampling errors. Least-squares regression was used to assess the relationships among the various relevant variables. Where appropriate, the decimal logarithm of the variable was regressed. The relationship equations, r^2, and p-value of the regressions are shown in the figure panels.

RESULTS
Temporal and Spatial Variability of Chlorophyll-*a* and Absorption
Figure 2a shows the average annual cycle of Chla-sat, absorption by phytoplankton, and absorption by CDOM+NAP calculated using MODIS eight-day composites for the period 2003–2016 for the whole SJG. Chla-sat and a_{phy} showed the same annual cycle. The spring bloom takes place in October (2.91 ±1.63 mg m^{-3}), followed by a long summer (December–March) with moderate Chla-sat concentrations (~2.00 mg m^{-3}). Finally, lower values are observed during winter (June–August; ~1.2 mg m^{-3}). The CDOM+NAP absorption showed less temporal variability with relatively higher values in winter and spring (~0.07–0.08 m^{-1}).

Table 1 shows the statistical variability of the in situ Chla and inherent optical properties at 440 nm (see online supplementary Table S1 for statistics at other wavelengths). The in situ Chla average value over the entire SJG was 1.34 ± 0.65 mg m^{-3}, corresponding to typical summer conditions but at the lower range of the climatological satellite value for February (1.95 ± 0.60 mg m^{-3}). Phytoplankton absorption contributes 66% of the particulate absorption at 440 nm.
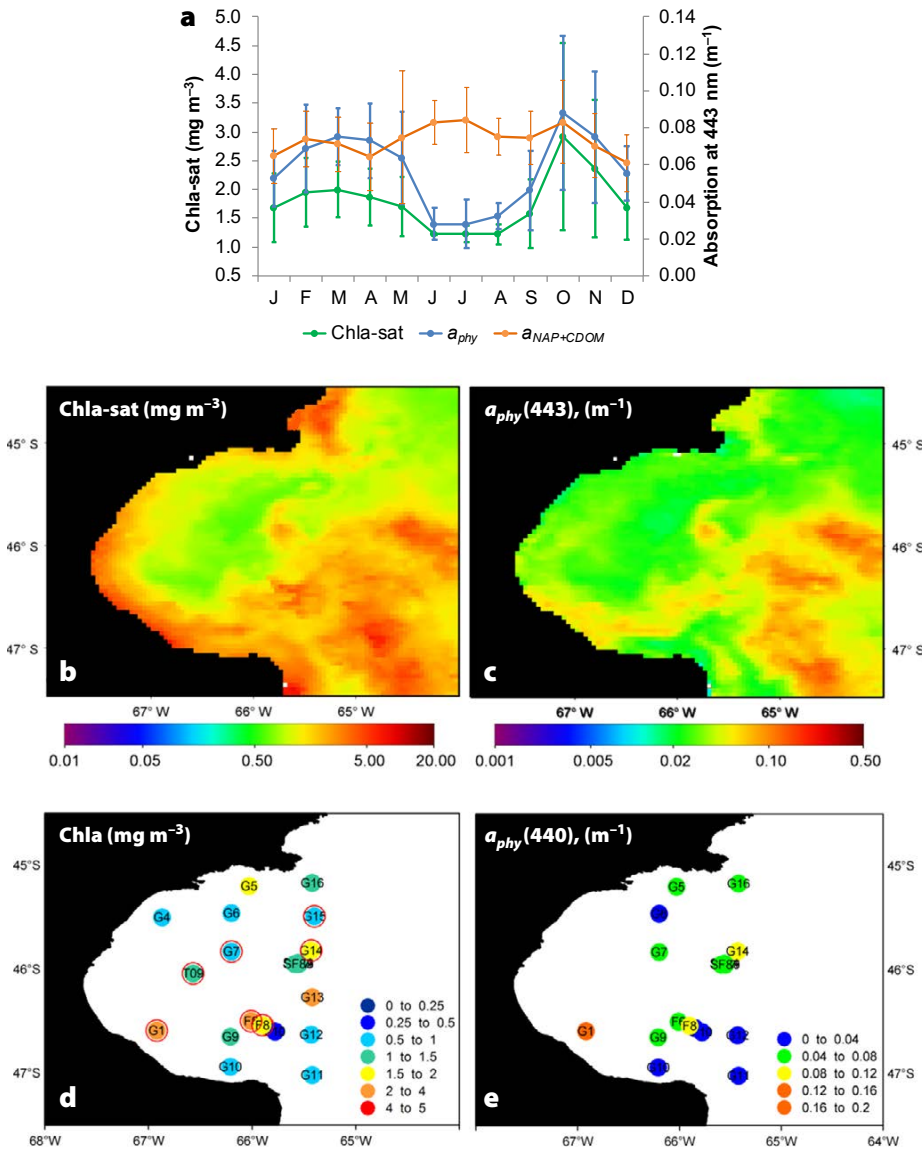
FIGURE 2. (a) Monthly satellite climatology of Chla, phytoplankton absorption a_{phy}(443), and non-algal particle colored dissolved organic matter $a_{CDOM+NAP}$(443) for the 2003–2017 period. Vertical bars are the standard deviations. February 2014 monthly satellite maps of (b) Chla and (c) a_{phy}(443). Spatial distribution of in situ surface (d) Chla and (e) a_{phy}(440).

TABLE 1. Ranges, means, standard deviations and variation coefficients of in situ surface (2 m depth) chlorophyll-*a* (Chla) concentrations (mg m^{-3}) and of absorption coefficients at 440 nm (m^{-1}) for colored dissolved organic matter (a_{CDOM}), particulate material (a_p), non-algal particles (a_{NAP}), phytoplankton (a_{phy}), and specific phytoplankton absorption (a_{phy}^*, m^2 mg^{-1}).

Water Constituents	Mean	Min	Max	SD	Variation Coefficient	N
Chla	1.32	0.29	2.70	0.65	0.49	25
a_{CDOM}(440)	0.15	0.03	0.36	0.12	0.80	6
a_p(440)	0.09	0.04	0.17	0.03	0.36	19
a_{NAP}(440)	0.03	0.02	0.09	0.02	0.54	19
a_{ph}(440)	0.06	0.01	0.13	0.03	0.50	19
a_{ph}^*(440)	0.05	0.01	0.08	0.01	0.20	19

Figure 2b,d shows that the highest in situ Chla concentrations (~2 mg m^{-3}) were measured close to the southeast (G13, F1, and F6) and southwest (G01) coasts. Stations with concentrations less than 1.5 mg m^{-3} were located mainly in the central and northern areas (G04, G06, and G07). This spatial variability is also seen in the average Chla-sat image for the cruise period (Figure 2b).

Figure 2c–e shows satellite-derived a_{phy} values at 443 nm for February 2014 and the spatial distribution of in situ measured IOPs at 440 nm (see Figure S1 for spatial distribution of in situ a_{NAP} and a_{CDOM} at 440 nm). In general, the in situ measurements agree relatively well with the satellite observations of the same variables, considering the strong spatial variability observed on the satellite images and the time gap between the in situ observations and the monthly average. The observed spatial patterns correspond well to the mesoscale features in the SJG as represented by the sea surface temperatures (Figure 1c).

Phytoplankton Community Composition

Figure 3 shows that the picophytoplankton size class dominated the density of the phytoplankton community over the SJG (mean of 2.02 ×10^7 cell L^{-1}). Nano-phytoplankton was the second group, with a mean of 1.7 × 106 cell L^{-1}. The micro-phytoplankton size class (diatoms and dinoflagellates) was poorly represented in the samples, with diatoms only detected in the northern area (G05), and dinoflagellates had a relatively uniform distribution throughout the SJG.

Absorption Budget

Table 2 shows the respective contributions of phytoplankton (a_{phy}), non-algal particles (a_{NAP}), and colored dissolved organic matter (a_{CDOM}) to total absorption (i.e., $a_p(\lambda) + a_{CDOM}(\lambda)$) at seven MODIS wavelengths. Only six stations met the condition of having simultaneous data of a_{phy}, a_{CDOM}, and a_{NAP}. At these stations, CDOM dominated light absorption at all

wavelengths except at 555 nm where it is similar to a_{NAP} as a result of the exponential decrease of a_{CDOM} with wavelength.

Figure 4 shows the relative contributions of absorption by phytoplankton, NAP, and CDOM at the seven MODIS wavelengths for all available stations. CDOM dominated the absorption at most stations except at G10 and G12, where NAP had a stronger impact on light absorption.

Phytoplankton Absorption

The absorption by particles showed two obvious absorption peaks around 440 nm and 675 nm (Figure 5a). Both peaks resulted from higher relative absorption by phytoplankton pigments (50%–70%; Figure 5b,c). NAP dominated the total particulate absorption ([($a_{NAP}(440)$/ $a_p(440)$] > 50%) between 540 nm and 630 nm (50%–70%). Figure 6a,b shows the regressions between a_{phy} at 440 nm and 675 mn and Chla. There are significant correlations at both wavelengths. The power function regression between $a_{phy}^*(\lambda)$ and Chla (y = ax^b) showed inverse correlations (Figure 6c–d), but with a relatively weak correlation coefficient (r^2 = 0.26) at the two wavelengths. The power function regressions between $a_{CDOM}(440)$ and $a_{phy}(440)$ and $a_{CDOM}(440)$ and $a_{phy}(675)$ show a significant, positive correlation despite the relatively small amount of data (Figure 6e,f).

DISCUSSION

Spatial Variability of Phytoplankton and Absorption by Different Components

The SJG annual cycle of Chla-sat is typical of temperate regions with seasonally stratified waters and two annual maximums (autumn and spring), minimum values in winter, and moderate values in summer (Glembocki et al., 2015). Therefore, the timing of the present cruise (between January 29 and February 15,
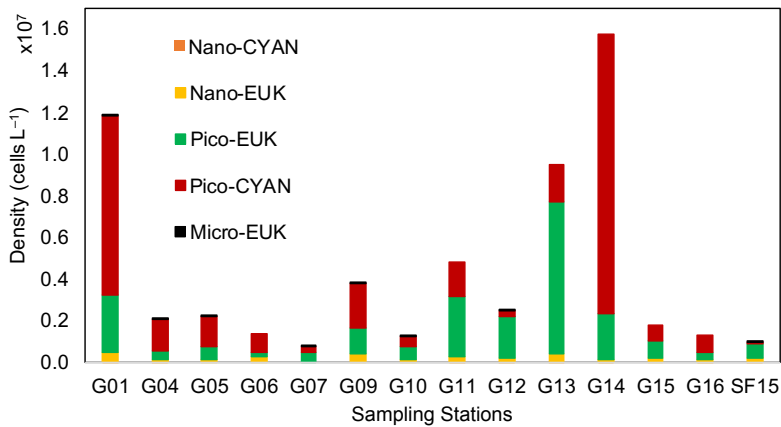
FIGURE 3. Phytoplankton density by size class and sampling station.

TABLE 2. Mean (standard deviation) of the relative contributions of $a_{phy}(\lambda)$, $a_{NAP}(\lambda)$, and $a_{CDOM}(\lambda)$ to total minus water absorption $a_{t-w}(\lambda)$ at the seven MODIS wavelengths (n = 6).

λ (nm)	$a_{phy}(\lambda)/a_{t-w}(\lambda)$	$a_{NAP}(\lambda)/a_{t-w}(\lambda)$	$a_{CDOM}(\lambda)/a_{t-w}(\lambda)$
412	0.14(0.05)	0.21(0.16)	0.65(0.18)
443	0.20(0.06)	0.21(0.17)	0.59(0.19)
469	0.22(0.06)	0.22(0.18)	0.56(0.21)
488	0.20(0.06)	0.22(0.15)	0.58(0.17)
531	0.14(0.03)	0.34(0.23)	0.51(0.23)
547	0.12(0.04)	0.35(0.21)	0.53(0.20)
555	0.11(0.04)	0.41(0.25)	0.48(0.24)
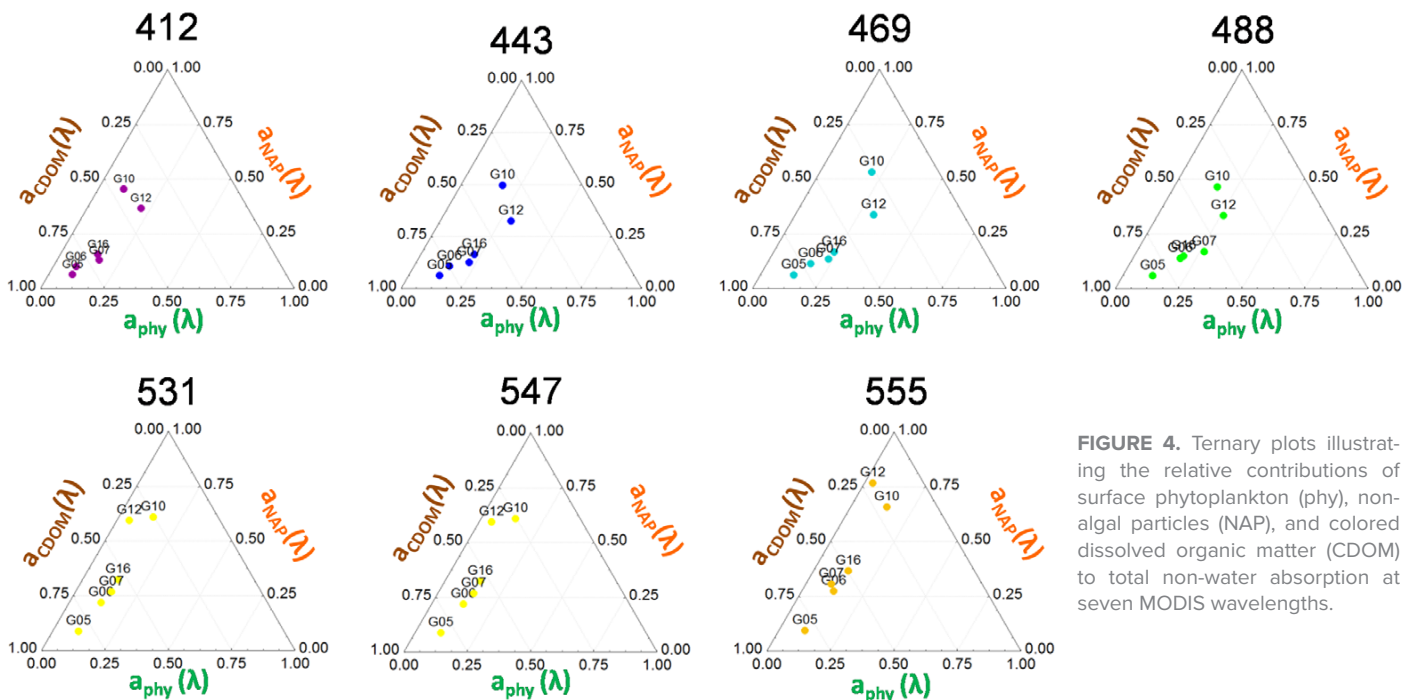
FIGURE 4. Ternary plots illustrating the relative contributions of surface phytoplankton (phy), non-algal particles (NAP), and colored dissolved organic matter (CDOM) to total non-water absorption at seven MODIS wavelengths.

2014) represents moderate phytoplankton biomass observed at the end of summer. Both the satellite image corresponding to the oceanographic cruise period (Figure 1b) and the in situ Chla data showed concentrations in the order of ~1.3 mg m^{-3} (Table 1).

The spatial distribution of Chla-sat and the main absorption components (Figure 2b,d) shows significant horizontal structures related to the general SJG oceanographic features (Figure 1c), including the influence of the Magellan Plume (Palma and Matano, 2012) in the southern sector and tidal fronts along the mouth and at the northeast end of the SJG (Glembocki et al., 2015). This spatial pattern is also consistent with previous observations of Chla and IOPs in the area (Segura et al., 2013a). The highest phytoplankton absorption values were observed at station G13 and G01 (~0.13 m^{-1}) associated with relatively high values of Chla (~ 2.0 mg m^{-3}) that in turn are related to small cells like picocyanobacteria and picoeukaryotes. Station G10 displayed maximum a_{NAP}(440) values (0.09 m^{-1}) that could be associated with the influence of the Magellan Plume (Palma and Matano, 2012; Lutz et al., 2016; Matano and Palma, 2018, in this issue) in the southern sector of the SJG mouth.

Absorption Budget

Results showed that light absorption by water constituents in the SJG was dominated by CDOM in summer (Table 2). CDOM may originate either from the degradation of phytoplankton cells and other organic particles in the water or from terrestrial sources (IOCCG, 2000). Usually, the former accounts for a higher percentage of CDOM in the open ocean, while the latter dominates in coastal, estuarine, and inland waters (Bricaud et al., 1981; Zhang et al., 2013). Also, CDOM can be released from bottom sediments during storm-driven suspension events (Boss et al., 2001). Figure 2a showed that, except during the winter season (May–September), there was a positive correlation between a_{phy} and $a_{CDOM+NAP}$ (r^2 = 0.53, S = 1.14, p <0.05, n = 26). This is corroborated by the in situ measurements at 440 nm and 675 nm (Figure 6e,f). Considering the small amount of terrestrial freshwater input to the SJG, this indicates that the CDOM components originate mainly from the degradation of phytoplankton cells and other organic particles during most of the year (IOCCG, 2000; Lutz et al., 2016).

Our results showed that phytoplankton are the main particulate absorbers (66%) as was previously observed in the area at the same season (70%, Segura et al., 2013a).

Particle and Phytoplankton Absorption

Xi et al. (2007) categorized the total particle absorption spectra into two types: one dominated by two obvious absorption peaks around 440 nm and 675 nm, and a second type in which a_{NAP} dominates, leading to only a slight absorption peak around 675 nm. Our analyses showed that during the summer in the SJG, most $a_p(\lambda)$ spectra belong to the first type, consistent with other observations made in the spring and summer at the Patagonia shelf break (Ferreira et al., 2009).

The specific absorption spectra $a_{phy}^{\star}$, being a measure of absorption efficiency per unit Chla (Kiefer and Mitchell, 1983; Berthon and Morel, 1992; Sakshaug et al., 1997), is a key parameter for estimating the amount of light absorbed by phytoplankton in bio-optical models of marine primary production. This parameter can also reflect the phytoplankton community's variations in cell size and pigment composition (Bricaud and Stramski, 1990), which are affected by regional and seasonal changes in species composition, light, and nutrient conditions (e.g., Lutz
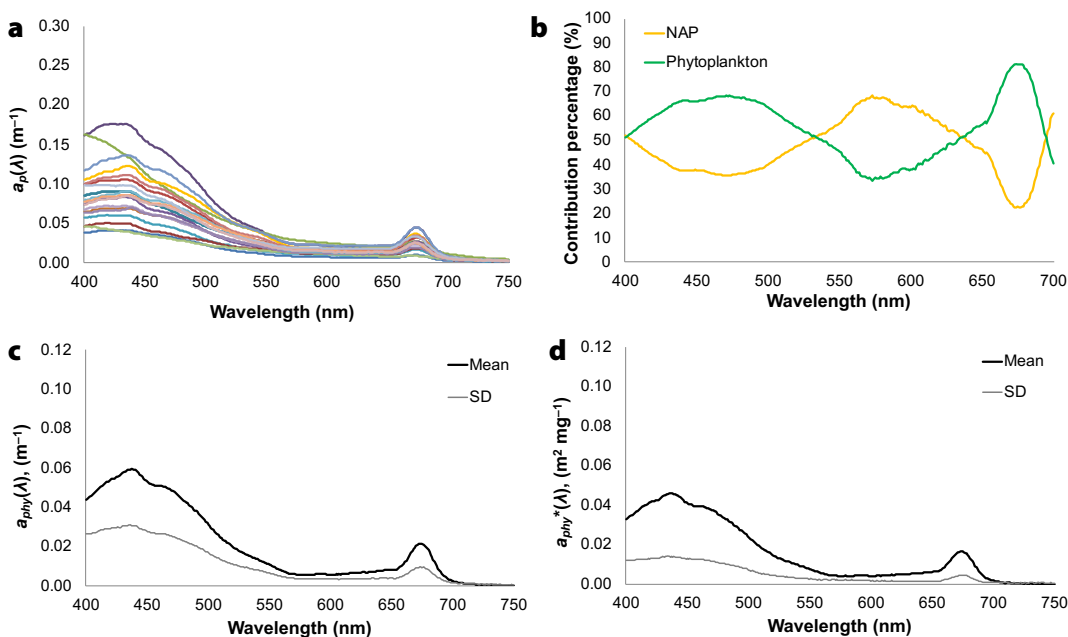
FIGURE 5. (a) Particle absorption spectra ($a_p(\lambda)$) and (b) percent contribution of NAP and phytoplankton to $a_p(\lambda)$. Plots of the mean and standard deviation (SD) of (c) phytoplankton absorption $a_{phy}(\lambda)$ and (d) chlorophyll-specific phytoplankton absorption $a_{phy}^{*}(\lambda)$ (n = 19).

et al., 1996; Stuart et al., 2000). Except at two stations (F1 and F6) where Chla was higher, leading to very small $a_{phy}{}^*(440)$ values, the $a_{phy}{}^*(440)$ measured at the end of summer in the SJG (0.01–0.08 m^2 mg^{-1}; Figure 6c) are in a similar range to those observed by Bricaud et al. (2004) for a variety of oceanic waters. The slope of the regression at 440 nm is also very similar to that found by Bricaud et al. (1995). The measured $a_{phy}{}^*(440)$ are also similar to those reported by Ferreira et al. (2009) at the Patagonian shelf break (0.044–0.11 m^2 mg^{-1}) for a community dominated by nano-phytoplankton and by Lutz et al. (2016) in Magellan Strait (0.018–0.069 m^2 mg^{-1}) for a community dominated by pico- and nano-phytoplankton. In our study, the density of the phytoplankton community was dominated by the picophytoplankton size class. Both a_{phy} and $a_{phy}{}^*$ spectra show the presence of a secondary peak at 450–480 nm (Figure 5c,d), which could be due to the presence of phytoplankton pigments other than chlorophyll-a (such as chlorophyll-b, β-carotene).

In this study, the exponent of the power function between in situ Chla and $a_{phy}(440)$ (b = 0.64) was close to those found by Bricaud et al. (1995, 2004) for large data sets, with Chla varying between 0.02 mg m^{-3} and 25 mg m^{-3} (0.65 < b < 0.73), but lower than that measured in summer (PATEX III cruise) at the Patagonia shelf break (b = 0.94) by Ferreira et al. (2009). Differences between the SJG $a_{phy}(440)$ values and those predicted by the regression of Bricaud et al. (1995, 2004) or observed by Ferreira et al. (2009) (Figure 6a,b) possibly result from differences in pigment compositions and cell sizes relative to what is typically found in other waters with similar Chla. Bricaud et al. (2004) indicated that the size structure of the algal population was the dominant cause of variations from the average a_{phy} vs. Chla relationship. In this sense, our results showed that the phytoplankton composition in the surface layer was mainly dominated by small cells (0.2–2 µm, i.e., picophytoplankton),
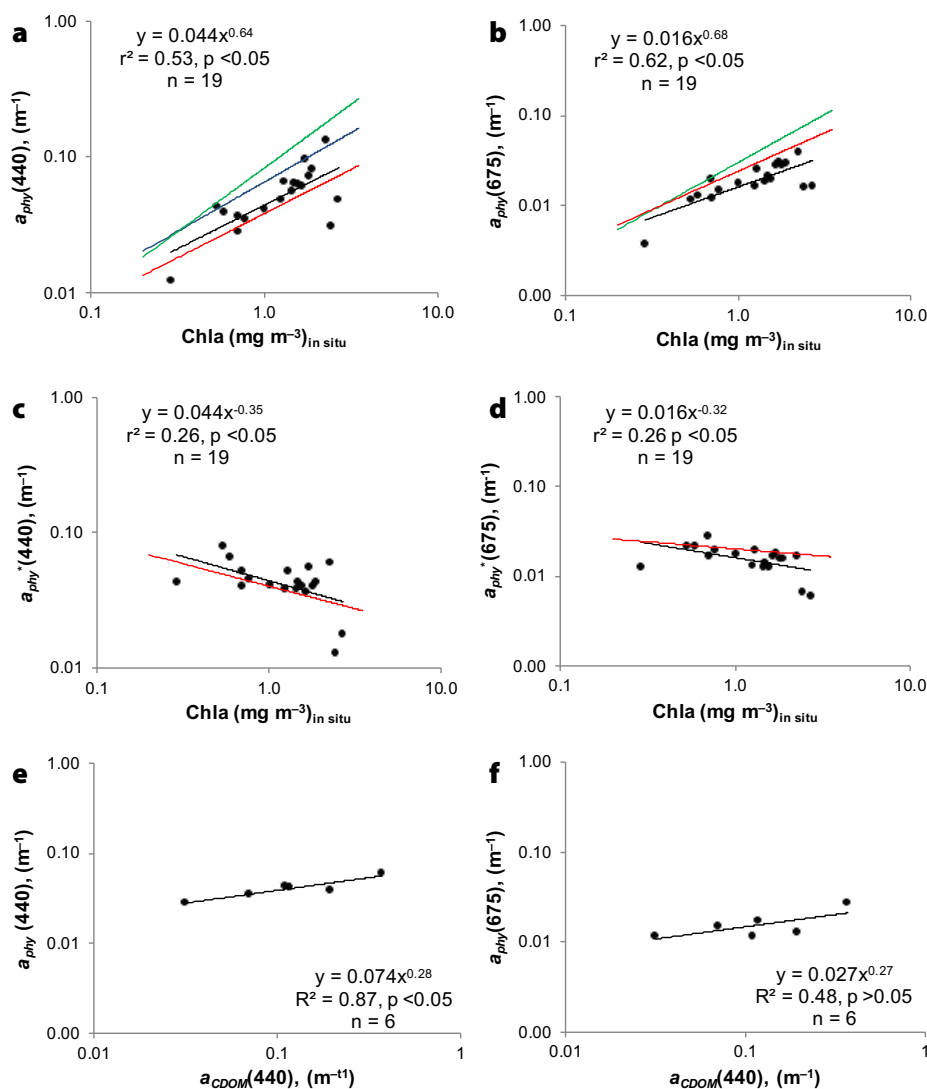
FIGURE 6. Scatterplots of in situ values of: (a,b) $a_{phy}(440)$ and $a_{phy}(675)$ vs. Chla; (c,d) $a_{phy}{}^*(440)$ and $a_{phy}{}^*(675)$ vs. Chla; (e) $a_{phy}(440)$ vs. $a_{CDOM}(440)$; and (f) $a_{phy}(675)$ vs. $a_{CDOM}(440)$. Regression lines for the data from this study and data from previous studies are shown, with current data in black, Bricaud et al. (1995) in red, Bricaud et al. (2004) in blue, and Ferreira et al. (2009) in green.

unlike that observed by Ferreira et al. (2009) at the Patagonia shelf-break, where the community was dominated by nanophytoplankton (2–20 µm) in summer. Another possible source of discrepancies with Bricaud et al. (2004) is that they used HPLC-derived pigment concentrations, which can differ markedly from fluorescence-derived Chla (Ferreira et al., 2009). As found elsewhere (Bricaud et al., 1995), the power function regression between $a_{phy}{}^*(440)$ and Chla shows inverse correlation but with a relatively weak coefficient. This possibly results from the spatial variability of phytoplankton species within the SJG in

summer associated with the presence of tidal fronts (Glembocki et al., 2015).

Another factor that can influence the relation between a_{phy} and in situ Chla is the pigment packaging effect, which can be evaluated using the $Q_a{}^*(675)$ indicator (Johnsen and Sakshaug, 2007; Roy et al., 2008). For the SJG, the calculated value is ~0.6, indicating a minimal packaging effect that is associated with more oligotrophic waters and dominance of small cells. At 440 nm, carotenoids, chlorophyll-b and -c, and phycobilins can contribute to the absorption, resulting in a specific absorption coefficient increase for a given in situ Chla concentration,

with important effects on the algorithm parameterization based only on the concentration of the main pigment (Lutz et al., 1996). The two phytoplankton pigment absorption peaks are often at the base of Chla algorithms in bio-optical models (Lee et al., 1998; Carder et al., 1999); thus, when developing regional-specific bio-optical algorithms, it is important to account for the seasonal variability of the $a_{phy}(\lambda)$ vs. the in situ Chla relationship (Xi et al., 2013).

CONCLUDING REMARKS

This study contributes to a better understanding of the annual phytoplankton cycle in San Jorge Gulf, a key coastal ecosystem in the Patagonian region. The general bio-optical characterization of the SJG showed the dominance of CDOM in the light absorption budget. The gulf is not a homogeneous water body, but rather displays large-scale spatial variability of Chla and inherent optical properties linked to the oceanic circulation and the bathymetry. This characterization is important for the assessment of ocean color algorithms and the estimation of primary production.

The good correlation between a_{CDOM} and a_{phy} indicates that the SJG can be classified within Case 1 oceanic waters, that is, with IOPs dominated by phytoplankton and related CDOM and detritus degradation products (Morel and Prieur, 1977; Gordon and Morel, 1983; Morel, 1988). Consequently, global remote-sensing algorithms should perform well in this area. Unfortunately, the limited set of in situ Chla data gathered during the survey did not allow a thorough validation of remote-sensing algorithms. More in situ data, especially from other seasons, would be necessary to perform that task. This study is a first step toward characterization of SJG optical properties. Future studies should also incorporate radiometric field data to evaluate atmospheric correction algorithms and acquire phytoplankton pigment composition information to better evaluate satellite algorithms. ©

REFERENCES

Acha, E.M., H.W. Mianzan, R.A. Guerrero, M. Favero, and J. Bava. 2004. Marine fronts at the continental shelves of austral South America. Physical and ecological processes. *Journal of Marine Systems* 44(1–2):83–105, https://doi.org/10.1016/j.jmarsys.2003.09.005.

Akselman, R. 1996. *Estudios ecológicos en el golfo San Jorge y adyacencias (Atlántico sudoccidental). Distribución, abundancia y variación estacional del fitoplancton en relación a factores físico-químicos y a la dinámica hidrográfica*. PhD Thesis, Universidad de Buenos Aires, Buenos Aires, Argentina.

Astoreca, R., D. Doxaran, K. Ruddick, V. Rousseau, and C. Lancelot. 2012. Influence of suspended particle concentration, composition and size on the variability of inherent optical properties of the Southern North Sea. *Continental Shelf Research* 35:117–128, https://doi.org/10.1016/j.csr.2012.01.007.

Berthon, J.F., and A. Morel. 1992. Validation of a spectral light-photosynthesis model and use of the model in conjunction with remotely sensed pigment observations. *Limnology and Oceanography* 37(4):781–796, https://doi.org/10.4319/lo.1992.37.4.0781.

Bogazzi, E., A. Baldoni, A.L. Rivas, P. Martos, R. Reta, J.M.L. Orensanz, M. Lasta, P. Dell' Arciprete, and F. Werner. 2005. Spatial correspondence between areas of concentration of Patagonian scallop (*Zygochlamys patagonica*) and frontal systems in the southwestern Atlantic. *Fisheries Oceanography* 14(5):359–376, https://doi.org/10.1111/j.1365-2419.2005.00340.x.

Boss, E., W.S. Pegau, J.R.V. Zaneveld, and A.H.B. Barnard. 2001. Spatial and temporal variability of absorption by dissolved material at a continental shelf. *Journal of Geophysical Research* 106:9,499–9,508, https://doi.org/10.1029/2000JC900008.

Bricaud, A., M. Babin, A. Morel, and H. Claustre. 1995. Variability in the chlorophyll-specific absorption coefficients of natural phytoplankton: Analysis and parameterization. *Journal of Geophysical Research* 100(C7):13,321–13,332, https://doi.org/10.1029/95JC00463.

Bricaud, A., H. Claustre, J. Ras, and K Oudbelkheir. 2004. Natural variability of phytoplanktonic absorption in oceanic waters: Influence of the size structure of algal populations. *Journal of Geophysical Research* 109(C11):1–12, https://doi.org/10.1029/2004JC002419.

Bricaud, A., A. Morel, and L. Prieur. 1981. Absorption by dissolved organic matter of the sea (yellow substance) in the UV and visible domains. *Limnology and Oceanography* 26(1):43–53, https://doi.org/10.4319/lo.1981.26.1.0043.

Bricaud, A., and D. Stramski. 1990. Spectral absorption coefficients of living phytoplankton and non-algal biogenous matter: A comparison between the Peru upwelling area and the Sargasso Sea. *Limnology and Oceanography* 53:562–582, https://doi.org/10.4319/lo.1990.35.3.0562.

Carder, K.L., F.R. Chen, Z.P. Lee, and S.K. Hawes. 1999. Semianalytic moderate resolution imaging spectrometer algorithms for chlorophyll *a* and absorption with bio-optical domains based on nitrate-depletion temperatures. *Journal of Geophysical Research* 104(C3):5,403–5,421, https://doi.org/10.1029/1998JC900082.

Carder, K.L., S.K. Hawes, K.A. Baker, R.C. Smith, R.G. Steward, and B.G. Mitchell. 1991. Reflectance model for quantifying chlorophyll *a* in the presence of productivity degradation products. *Journal of Geophysical Research* 96(C11):20,599–20,611, https://doi.org/10.1029/91JC02117.

Carreto, J.I., M.O. Carignan, N.G. Montoya, and D.A. Cucchi Colleoni. 2007. Ecología del fitoplancton en los sistemas frontales del Mar Argentino. Pp.11–31 in *El Mar Argentino y sus recursos Pesqueros El ambiente Marino Tomo V*. J.I. Carreto, and C. Bremec, eds, INIDEP, Mar del Plata, 169 pp.

Collier, J.L. 2000. Flow cytometry and the single cell in phycology 1. *Journal of Phycology* 36(4):628–644, https://doi.org/10.1046/j.1529-8817.2000.99215.x.

Cucchi Colleoni, A.D., and J.I. Carreto. 2001. *Variación estacional de la biomasa fitoplanctónica en el golfo San Jorge. Resultados de las campañas de investigación: OB-01/00, OB-03/00, OB-10/00, y OB-12/00*. INIDEP Informe Técnico Interno N°49, 30 pp.

Fernández, M. 2006. *Características físico-químicas de los sedimentos del Golfo San Jorge y su relación con los organismos bentónicos del sector*. PhD Thesis. Universidad Nacional de Mar del Plata, Mar del Plata, Argentina.

Fernández, M., J.I. Carreto, J. Mora, and A. Roux. 2005. Physico-chemical characterization of the benthic environment of the Golfo San Jorge, Argentina. *Journal of the Marine Biological Association of the United Kingdom* 85:1,317–1,328, https://doi.org/10.1017/S002531540501249X.

Fernández, M., A. Roux, E. Fernández, J. Caló, A. Marcos, and H. Aldacur. 2003. Grain-size analysis of surficial sediments from Golfo San Jorge, Argentina. *Journal of the Marine Biological Association of the United Kingdom* 83:1,193–1,197, https://doi.org/10.1017/S0025315403008488.

Ferreira, A., V.M.T. García, and C.A.E. García. 2009. Light absorption by phytoplankton, non-algal particles and dissolved organic matter at the Patagonia shelf-break in spring and summer. *Deep Sea Research Part I* 56(12):2,162–2,174, https://doi.org/10.1016/j.dsr.2009.08.002.

Gagliardini, D.A., and P.C. Colón. 2004. Ocean feature detection using microwave backscatter and sun glint observations. *Gayana* 68(2):180–185, https://doi.org/10.4067/S0717-65382004000200033.

Garcia, C., V. Garcia, and C. McClain. 2005. Evaluation of SeaWiFS chlorophyll algorithms in the Southwestern Atlantic and Southern Oceans. *Remote Sensing of Environment* 95(1):125–137, https://doi.org/10.1016/j.rse.2004.12.006.

Glembocki, N.G., G.N. Williams, M.E. Góngora, D.A. Gagliardini, and J.M. (Lobo) Orensanz. 2015. Synoptic oceanography of San Jorge Gulf (Argentina): A template for Patagonian red shrimp (*Pleoticus muelleri*) spatial dynamics. *Journal of Sea Research* 95:22–35, https://doi.org/10.1016/j.seares.2014.10.011.

Gordon, H., and A. Morel. 1983. *Remote Assessment of Ocean Color for Interpretation of Satellite Visible Imagery*, vol. 4. Springer-Verlag, and published by the American Geophysical Union as part of the Lecture Notes on Coastal and Estuarine Studies Series, 114 pp., https://doi.org/10.1029/LN004.

Hancke, K., E.K. Hovland, Z. Volent, R. Pettersen, G. Johnsen, M. Moline, and E. Sakshaug. 2014. Optical properties of CDOM across the Polar Front in the Barents Sea: Origin, distribution and significance. *Journal of Marine Systems* 130:219–227, https://doi.org/10.1016/j.jmarsys.2012.06.006.

Hoepffner, N., and S. Sathyendranath. 1992. Bio-optical characteristics of coastal waters: Absorption spectra of phytoplankton and pigment distribution in the western North Atlantic. *Limnology and Oceanography* 37(8):1,660–1,679, https://doi.org/10.4319/lo.1992.37.8.1660.

Hudson, N., A. Baker, D.M. Reynolds, C. Carliell-Marquest, and D. Ward. 2009. Changes in freshwater organic matter fluorescence intensity with freezing/thawing and dehydration/rehydration. *Journal of Geophysical Research* 114, G00F08, https://doi.org/10.1029/2008JG000915.

IOCCG (International Ocean-Colour Coordinating Group). 2000. *Remote Sensing of Ocean Colour in Coastal and Other Optically-Complex Waters*.

S. Sathyendranath, ed., Reports of the International Ocean-Colour Coordinating Group, No. 3, IOCCG, Dartmouth, Canada, 140 pp.

IOCCG. 2006. *Remote Sensing of Inherent Optical Properties: Fundamentals, Tests of Algorithms, and Applications.* Z.P. Lee, ed., Reports of the International Ocean-Colour Coordinating Group, No. 5, IOCCG, Dartmouth, Canada, 126 pp., https://doi.org/10.25607/OBP-96.

Johnsen, G., and E. Sakshaug. 2007. Biooptical characteristics of PSII and PSI in 33 species (13 pigment groups) of marine phytoplankton, and the relevance for pulse amplitude-modulated and fast-repetition-rate fluorometry. *Journal of Phycology* 43:1,236–1,251, https://doi.org/10.1111/j.1529-8817.2007.00422.x.

Kiefer, D.A., and B.G. Mitchel. 1983. A simple, steady-state model of phytoplankton production based on absorption cross-section and quantum efficiency. *Limnology and Oceanography* 27:492–499, https://doi.org/10.4319/lo.1983.28.4.0770.

Kishino, M., N. Takahashi, N., Okami, N.S. Ichimura. 1985. Estimation of the spectral absorption coefficient of phytoplankton in the sea. *Bulletin of Marine Science* 37:634–642.

Lee, Z., K.L. Carder, C.D. Mobley, R.G. Steward, and J.S. Patch. 1998. Hyperspectral remote sensing for shallow waters. I. A semi-analytical model. *Applied Optics* 37(27):6,329–6,338, https://doi.org/10.1364/AO.37.006329.

Lutz, V., R. Frouin, R. Negri, R. Silva, M. Pompeu, N. Rudorff, A. Cabral, A. Dogliotti, and G. Martínez. 2016. Bio-optical characteristics along the Straits of Magallanes. *Continental Shelf Research* 119:56–67, https://doi.org/10.1016/j.csr.2016.03.008.

Lutz, V.A., S. Sathyendranath, and E.J.H. Head. 1996. Absorption coefficient of phytoplankton: Regional variations in the North Atlantic. *Marine Ecology Progress Series* 135:197–213, https://doi.org/10.3354/meps135197.

Lutz, V.A., A. Subramaniam, R.M. Negri, R.I. Silva, and J.I. Carreto. 2006. Annual variations in bio-optical properties at the "Estación Permanente de Estudios Ambientales (EPEA)" coastal station, Argentina. *Continental Shelf Research* 26(10):1,093–1,112, https://doi.org/10.1016/j.csr.2006.02.012.

Matano, R.P., and E.D. Palma. 2018. Seasonal variability of the oceanic circulation in the Gulf of San Jorge, Argentina. *Oceanography* 31(4):16–24, https://doi.org/10.5670/oceanog.2018.402.

Mitchell, B.G. 1990. Algorithms for determining the absorption coefficient of aquatic particulates using the quantitative filter technique (QFT). Pp. 137–148 in *Proceedings of SPIE, vol. 1302, Ocean Optics X*, https://doi.org/10.1117/12.21440.

Mitchell, B.G., and D.A. Kiefer. 1988. Variability in pigment specific particulate fluorescence and absorption spectra in the northeastern Pacific Ocean. *Deep Sea Research Part A* 35:665–689, https://doi.org/10.1016/0198-0149(88)90025-8.

Morel, A. 1988. Optical modeling of the upper ocean in relation to its biogeneous matter content (Case 1 waters). *Journal of Geophysical Research* 93(C9):10,749–10,768, https://doi.org/10.1029/JC093iC09p10749.

Morel, A., and L. Prieur. 1977. Analysis of variations in ocean color. *Limnology and Oceanography* 22(4):709–722, https://doi.org/10.4319/lo.1977.22.4.0709.

Nelson, N.B., and P.G. Coble. 2009. Optical analysis of CDOM. Pp. 79–96 in *Practical Guidelines for the Analysis of Seawater*. O. Wurl, ed., CRC Press.

Palma, E.D., and R.P. Matano. 2012. A numerical study of the Magellan Plume. *Journal of Geophysical Research* 117(C5), C05041, https://doi.org/10.1029/2011JC007750.

Preisendorfer, R.W. 1976. *Hydrologic Optics, Vol. 1: Introduction*. U.S. Department of Commerce, National Oceanic & Atmospheric Administration, Environmental Research Laboratories, Honolulu, Hawaii, 258 pp.

Prieur, L., and S. Sathyendranath. 1981. An optical classification of coastal and oceanic waters based on the specific spectral absorption curves of phytoplankton pigments, dissolved organic matter, and other particulate materials. *Limnology and Oceanography* 26(4):671–689, https://doi.org/10.4319/lo.1981.26.4.0671.

Rivas, A.L. 2006. Quantitative estimation of the influence of surface thermal fronts over chlorophyll concentration at the Patagonian shelf. *Journal of Marine Systems* 63(3–4):183–190, https://doi.org/10.1016/j.jmarsys.2006.07.002.

Rivas, A.L., and J.P. Pisoni. 2010. Identification, characteristics and seasonal evolution of surface thermal fronts in the Argentinean Continental Shelf. *Journal of Marine Systems* 79(1–2):134–143, https://doi.org/10.1016/j.jmarsys.2009.07.008.

Roesler, C.S., and M.J. Perry. 1995. In situ phytoplankton absorption, fluorescence emission, and particulate backscattering spectra determined from reflectance. *Journal of Geophysical Research* 100(C7):13,279–13,294, https://doi.org/10.1029/95JC00455.

Romero, S.I., A.R. Piola, M. Charo, and C.A. Eiras Garcia. 2006. Chlorophyll-*a* variability off Patagonia based on SeaWiFS data. *Journal of Geophysical Research* 111(5):1–11, https://doi.org/10.1029/2005JC003244.

Roy, S., F. Blouin, A. Jacques, and J.C. Therriault. 2008. Absorption properties of phytoplankton in the lower estuary and Gulf of St. Lawrence (Canada). *Canadian Journal of Fisheries and Aquatic Sciences* 65(8):1,721–1,737, https://doi.org/10.1139/F08-089.

Sakshaug, E., A. Bricaud, Y. Dandonneau, P.G. Falkowski, D.A. Kiefer, L. Legendre, L. Legendre, A. Morel, J. Parslow, and M. Takahashi. 1997. Parameters of photosynthesis: Definitions, theory and interpretation of results. *Journal of Plankton Research* 19:1637–1670, https://doi.org/10.1093/plankt/19.11.1637.

Segura, V., D. Cuchi Colleoni, and V.A. Lutz. 2013a. *Características Bio-ópticas del Material Particulado Total y Su Relación con la Clorofila-a en el Golfo San Jorge y Área Adyacente: Campañas OB03/2008 y OB/2009*. Informe Técnico Nro. 076, Instituto Nacional de Desarrollo Pesquero, Mar del Plata (Argentina), 19 pp.

Segura, V., V. Lutz, A. Dogliotti, R. Silva, R. Negri, R. Akselman, and H. Benavides. 2013b. Phytoplankton types and primary production in the Argentine Sea. *Marine Ecology Progress Series* 491:15–31, https://doi.org/10.3354/meps10461.

Spencer, R.G.M., L. Bolton, and A. Baker. 2007. Freeze/thaw and pH effects on freshwater dissolved organic matter fluorescence and absorbance properties from a number of UK locations. *Water Research* 41:2,491–2,950, https://doi.org/10.1016/j.watres.2007.04.012.

Spencer, R.G.M., and P.G. Coble. 2014. Sampling design for organic matter analysis. Pp. 125–146 in *Aquatic Organic Matter Fluorescence*. P.G. Coble, J. Lead, A. Baker, D.M. Reynolds, and R.G.M. Spencer, eds, Cambridge University Press.

Strickland, J.D.H., and T.R. Parsons. 1972. *A Practical Handbook of Seawater Analysis*. Fisheries Research Board of Canada, Bulletin 167, Ottawa, 310 pp.

Stuart, V., S. Sathyendranath, E.J.H. Head, T. Platt, B. Irwin, and H. Maass. 2000. Bio-optical characteristics of diatoms and prymnesiophyte populations in the Labrador Sea. *Marine Ecology Progress Series* 201:91–106, https://doi.org/10.3354/meps201091.

Tomas, C.R. 1997. *Identifying Marine Phytoplankton*. Academic Press, 875 pp.

Tremblay, G., C. Belzile, M. Gosselin, M. Poulin, S. Roy, and J.É. Tremblay. 2009. Late summer phytoplankton distribution along a 3500 km transect in Canadian Arctic waters: Strong numerical dominance by picoeukaryotes. *Aquatic Microbial Ecology* 54(1):55–70, https://doi.org/10.3354/ame01257.

Utermöhl, H. 1958. Zur Vervollkommnung der quantitativen Phytoplankton-Methodik: Mit 1 Tabelle und 15 abbildungen im Text und auf 1 Tafel. *Internationale Vereinigung Für Theoretische Und Angewandte Limnologie: Mitteilungen* 9(1):1–38.

Xi, H., P. Larouche, S. Tang, and C. Michel. 2013. Seasonal variability of light absorption properties and water optical constituents in Hudson Bay, Canada. *Journal of Geophysical Research* 118(6):3,087–3,102, https://doi.org/10.1002/jgrc.20237.

Xi, H., Z. Qiu, Y. He, and Jian W. 2007. The absorption of water color components and spectral modes in the Pearl River estuary. *Chinese Journal of Oceanology and Limnology* 25(4):359–366, https://doi.org/10.1007/s00343-007-0359-3.

Zhang, Y., X. Liu, M. Wang, and B. Qin. 2013. Compositional differences of chromophoric dissolved organic matter derived from phytoplankton and macrophytes. *Organic Geochemistry* 55:26–37, https://doi.org/10.1016/j.orggeochem.2012.11.007.

ACKNOWLEDGMENTS

AUTHORS

Gabriela N. Williams (williams@cenpat-conicet.gob.ar) is a researcher at the Centro para el Estudio de Sistemas Marinos (CESIMAR), Centro Científico Tecnológico (CCT), Consejo Nacional de Investigaciones Científicas y Técnicas (CONICET)-Centro Nacional Patagónico (CENPAT), Puerto Madryn, Chubut, Argentina. **Pierre Larouche** is an emeritus scientist at the Institut Maurice Lamontagne, Mont-Joli, and Associate Professor at the Institut des sciences de la mer de Rimouski, Université du Québec à Rimouski, Québec, Canada. **Ana I. Dogliotti** is a researcher at the Instituto de Astronomía y Física del Espacio, Universidad de Buenos Aires, CONICET Buenos Aires, Ciudad Autónoma de Buenos Aires, Argentina. **Maité P. Latorre** is a PhD candidate at CESIMAR, CCT, CONICET-CENPAT, Puerto Madryn, Chubut, Argentina.

ARTICLE CITATION